Journal of
Nanoscience and Nanotechnology
Vol. 8, 1443–1448, 2008

Study on UV Excitation Properties of $Y_2O_3:Ln^{3+}$ (Ln = Eu^{3+} or Tb^{3+}) Luminescent Nanomaterials

Qingyu Meng[1,2], Baojiu Chen[1,3,*], Xiaoxia Zhao[1,2], Xiaojun Wang[1], and Wu Xu[1,4]

[1]Key Laboratory of Excited State Processes, Changchun Institute of Optics, Fine Mechanics and Physics, Chinese Academy of Sciences, Changchun 130033, P. R. China
[2]Graduate School of the Chinese Academy of Sciences, Beijing 100039, P. R. China
[3]Department of Physics, Dalian Maritime University, Dalian 116026, P. R. China
[4]University of Science and Technology of China, Hefei 230026, P. R. China

$Y_2O_3:Ln^{3+}$ (Ln = Eu or Tb) nanocrystals with different Ln^{3+} doping concentrations and average sizes were prepared by chemical self-combustion. The corresponding bulk materials with various doping concentrations were obtained by annealing the nanomaterials at high temperature. The emission spectra, excitation spectra, and X-ray diffraction spectra were used in this study. It was found that the charge transfer band of $Y_2O_3:Eu^{3+}$ red-shifted as particle size decreased, and the charge transfer band in the 5-nm particles obviously broadened toward the long wavelength. It was also found that the profile of excitation spectra corresponding to the $4f5d$ ($4f^8 \rightarrow 4f^75d^1$) transition changed a lot with the variation of the particle size. The dependence of the excitation spectra of $Y_2O_3:Ln^{3+}$ on particle size was investigated.

Keywords: $Y_2O_3:Ln^{3+}$ (Ln = Eu or Tb) Nanomaterials, UV Excitation, Surface, Exciton Absorption.

RESEARCH ARTICLE

1. INTRODUCTION

Rare earths (RE) doped inorganic materials have been widely used in applications such as displays, lighting, optical communication, and laser devices. These luminescent materials have attracted extensive interest.[1] With the development of the display technique, the demand for high resolution display screens is also increasing. Nanophosphors would be helpful for improving display resolution. Also, because nanomaterials have special properties that are different from the bulk materials there has been much interest in exploring the elemental physical mechanisms causing the differences between nano and bulk materials and in finding potential applications as new engineering materials in many aspects relative to the luminescence.[1–3] However, most previous literature has reported that nanophosphors have low luminescence efficiency and low quantum efficiency that has been attributed to the influence of surface state and quantum dimension confinement. The low luminescent yields of nanomaterials restrict their practical applications. Thus, further study on the surface state effect, quantum dimension effect, and quantum confinement effect in RE-doped nanophosphors will increase our understanding of the factors influencing the growth of luminescent yields, and furthermore, aid in the design of new materials for our purposes.[1,4,5]

As mature commercialized red and green phosphors, $Y_2O_3:Eu^{3+}$ and $Y_2O_3:Tb^{3+}$ have been extensively studied. The excitation spectrum of $Y_2O_3:Eu^{3+}$ is composed of a charge transfer band and that of $Y_2O_3:Eu^{3+}$ is composed of the $4f5d$ transition in the UV region, which match the excitation light wavelengths. Thereby, the research on the charge transfer (CT) band and the $4f5d$ transition is meaningful in the interest of improving luminescent properties of the nanomaterials.

2. EXPERIMENTAL DETAILS

The $Y_2O_3:Ln^{3+}$ (Ln = Eu or Tb) nanocrystal powders studied in this work were prepared by chemical auto-combustion. The detailed preparative procedure has been reported previously in the literature. Here, we present the main experimental steps. First, $Y(NO_3)_3$, $Ln(NO_3)_3$, and glycine solution were mixed to form the precursor solution. The precursor solution was heated to evaporate all the water and then burned. The resulting products

*Author to whom correspondence should be addressed.

1533-4880/2008/8/1443/006 doi:10.1166/jnn.2008.363

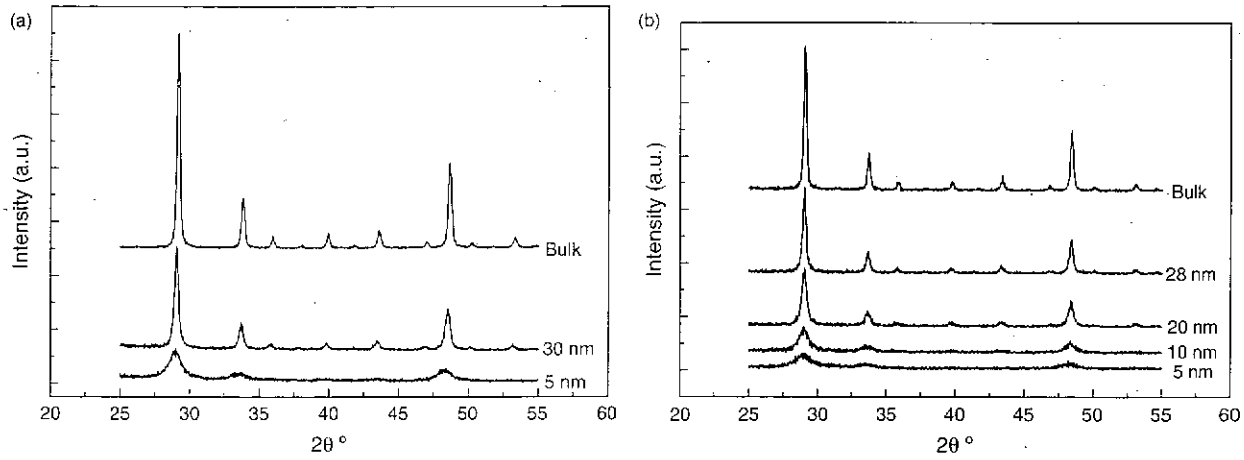

Fig. 1. (a) XRD spectra of Y_2O_3:Eu^{3+} samples of different sizes. (b) XRD spectra of Y_2O_3:Tb^{3+} samples of different sizes.

were Y_2O_3:Ln^{3+} nanocrystal powders, where the doping concentration of Ln ions is expressed by the relation [Y]:[Ln] = $(1 - X)$:X. The nanoparticle sizes were controlled by changing the dosage of glycine. In order to increase the crystallinity, the combustion products were annealed at 500 °C for 1 h, and the Y_2O_3:Tb^{3+} nanocrystals were annealed in a carbon powder reductive atmosphere to avoid the oxidation of Tb^{3+}. It is known that short duration annealing at 500 °C will hardly affect the size of the nanoparticles, and all the samples in this study were annealed. The bulk Y_2O_3:Ln^{3+} crystals were obtained by annealing the nanocrystals at 1,000 °C for 6 h.

The excitation and emission spectra were measured using a HITACHI F-4500 fluorescent spectrophotometer

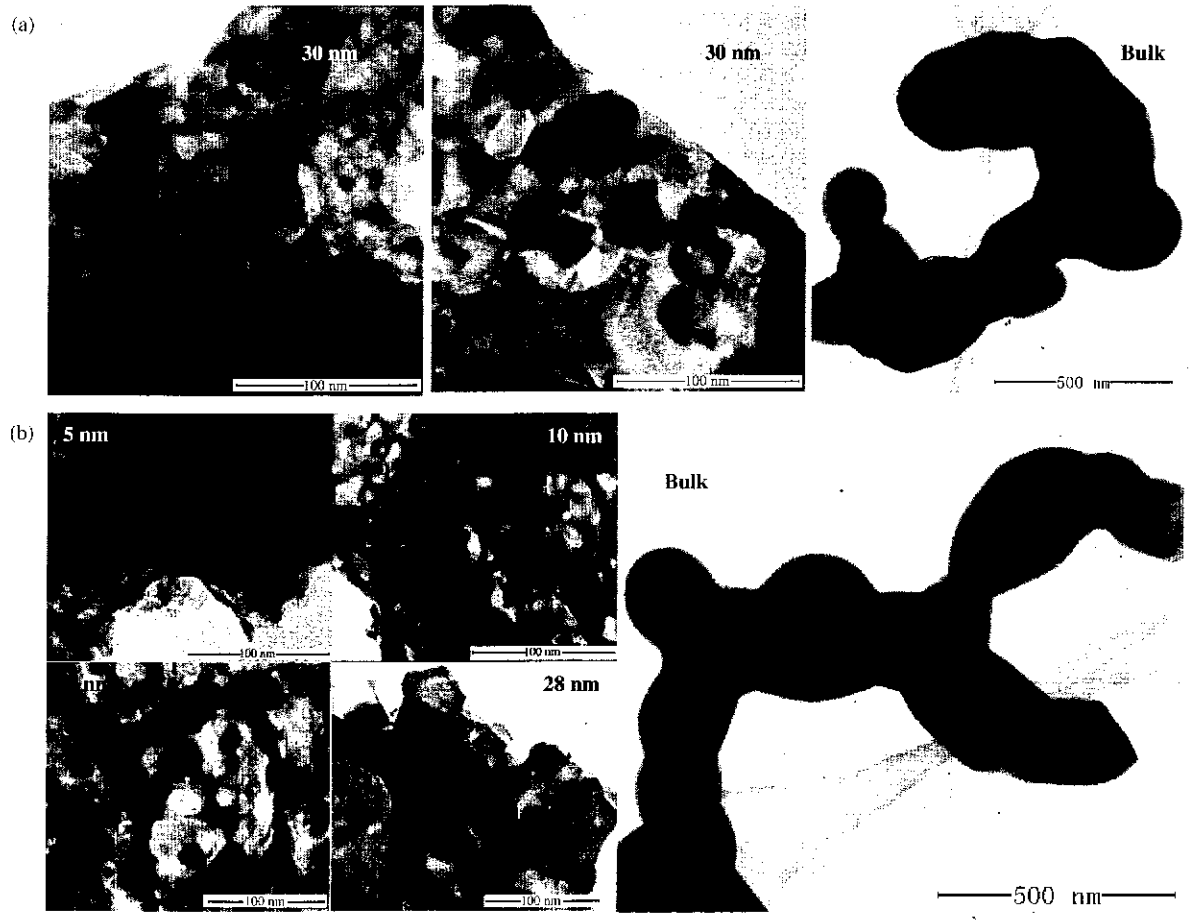

Fig. 2. (a) TEM image of Y_2O_3:Eu^{3+} samples with different particle sizes. (b) TEM image of Y_2O_3:Tb^{3+} for the samples with different particle sizes.

equipped with a 200 W xenon lamp as the excitation source. The X-ray diffraction (XRD) patterns were measured with a Rigaku D/max-II B X-ray diffractometer.

The XRD patterns for the Y_2O_3:Eu^{3+} and Y_2O_3:Tb^{3+} samples with various particle sizes are shown in Figures 1(a) and (b), respectively. From these figures, it can be seen that all the resultant Y_2O_3:Ln^{3+} particles exist in the cubic phase. The average particle sizes were approximated by the Scherrer formula:

$$D = k\lambda/[(\beta^2 - \beta_0^2)^{1/2}\cos\theta] \quad (1)$$

where k is 0.9, λ (1.54 angstroms) is the α-radiation wavelength of the copper target, β represents the full width at half maximum (FWHM) of the diffraction peak, β_0 is a modification factor for the system broadening, and θ stands for the half of the diffraction position 2θ. The average sizes of the Y_2O_3:Eu^{3+} samples are estimated to be 5 nm, 15 nm, 30 nm, and larger then 100 nm for the sample annealed at high temperature. For Y_2O_3:Tb^{3+} samples, the sizes are 5 nm, 10 nm, 20 nm, 28 nm, and larger than 100 nm for the sample annealed at high temperature.

Figures 2(a) and (b) show the TEM images for the corresponding samples in Figures 1(a) and (b). It is seen that the particle sizes exhibited by TEM are in good agreement with the calculation derived from XRD.

3. RESULTS AND DISCUSSION

3.1. The O → Eu Charge Transfer Band of Y_2O_3:Eu^{3+} Nanocrystallines

Figure 3 shows the normalized excitation spectra of Y_2O_3:Eu^{3+} (doping concentration $X = 0.01$) crystals with different particle sizes, while monitoring the 611 nm emission of the Eu^{3+} $^5D_0 \rightarrow {}^7F_2$ transition. The 200–220 nm band corresponds to the host absorption band of Y_2O_3 (exciton absorption).[6,7] The 220–280 nm band corresponds with the charge transfer band of O → Eu. Figure 3 shows

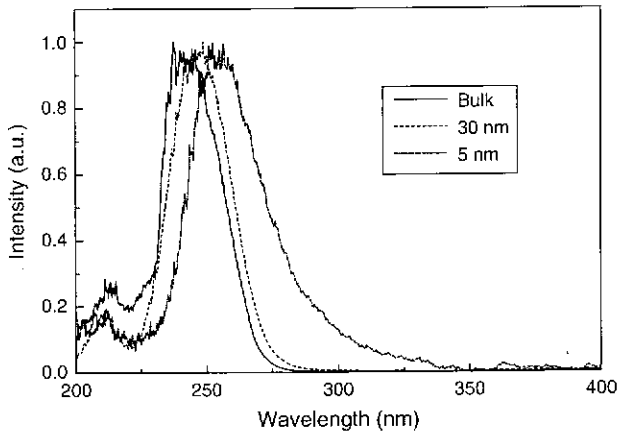

Fig. 3. Excitation spectra of Y_2O_3:Eu^{3+} of different sizes, monitoring the 611 nm emission of $^5D_0 \rightarrow {}^7F_2$ transition of Eu^{3+} ($X = 0.01$).

that the host absorption band slightly blue-shifts with the decrease in particle size. This shift indicates the broadening of the band gap between the valence band and the conduction band of the host Y_2O_3 with the decrease in particle size. It is also observed in Figure 3 that the charge transfer band obviously red-shifts with the decrease in particle size, and the CT band of the 5-nm sample broadens toward the long wavelength. The red shift can be explained as follows. As the particle size decreases, the lattice constant increases, the bond length between O^{2-} and Eu^{3+} increases, and the bond energy decreases, then the CT transition energy decreases.[8] The O → Eu band energy in the low crystallinity environment is lower than that in the high crystallinity environment, so that the CT band of Eu^{3+} in the low crystallinity environment is located at the long wavelengths. As the particle size decreases, the ionic number of Eu^{3+} located at or near the surface in the low crystallinity environment increases; therefore the broadened CT band for the 5-nm sample includes both the contributions from the Eu^{3+} ions at or near the particle surface and from the Eu^{3+} ions inside the nanoparticle.[9,10] From this point, the quantum dimension effect can be used to control the location of the CT band.

3.2. The *4f5d* Transition of Tb^{3+} in Y_2O_3:Tb^{3+} Nanocrystals

In recent years, various Tb^{3+}-doped host materials have been widely studied, but less attention has been paid to the $4f5d$ transition.[4,11–13] It is well known that the $4f5d$ transitions are different from the transitions in the intra-$4f^n$ configurations since the $4f$-electrons are shielded by the $5s$ and $5p$ closed-shell electrons. The $4f5d$ transitions are more sensitive to the local environment surrounding the Tb^{3+} ions than the $f-f$ transitions. Nanoparticles possess large surface area-to-volume ratio and low crystallinity that may cause a change of the $4f5d$ transition of Tb^{3+}.

Figure 4 depicts the excitation spectra of Y_2O_3:Tb^{3+} ($X = 0.01$) nanocrystals with different particle sizes, monitoring the 543 nm green fluorescence emission of the $^5D_0 \rightarrow {}^7F_5$ transition. The 210 nm excitation band corresponds to the host absorption band of Y_2O_3. The 220–230 nm excitation band corresponds to the $4f^8 \rightarrow 4f^75d^1$ (^8S) transition absorption band[7,15,16] whose energy is the lowest among the $4f5d$ transitions of Tb^{3+}. Figure 4 shows that the spectral line shape of the $4f5d$ transition changes a lot when particle size increases. For the sample with particle size of 5 nm, the excitation spectra exhibit a broad band composed of three peaks: an intense peak at 235 nm and two weak peaks at 273 and 303 nm. As particle size increases, the intensity of the excitation peak at 235 nm decreases, and the intensity of the peaks at 273 and 303 nm increases. For the samples with particle size of 28 nm, the excitation peak at 235 nm is difficult to distinguish, and its spectral line shape is similar to that of the bulk material. This variety can be attributed

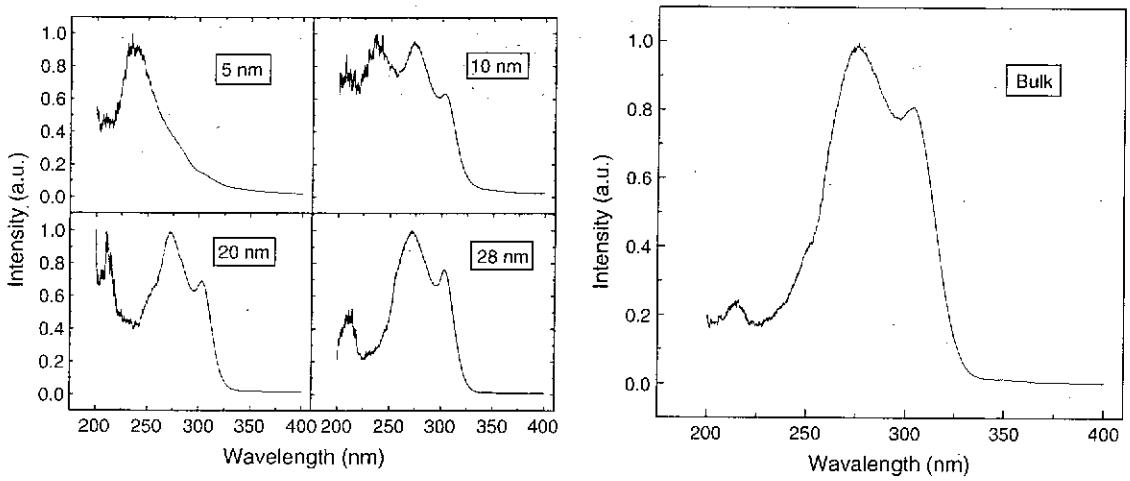

Fig. 4. Excitation spectra of Y_2O_3:Tb^{3+} of different sizes, monitoring the 543 nm emission of the $^5D_4 \rightarrow {}^7F_5$ transition of Tb^{3+} ($X = 0.01$).

to the change in the environment where the Tb^{3+} ions are located. As mentioned above, the $4f5d$ transitions are sensitive to environment. Compared with the bulk materials, the Tb^{3+} in nanomaterials may occupy complicated sites due to their large surface area-to-volume ratio. The excitation peak at 235 nm corresponds to the $4f5d$ transition of Tb^{3+} ions located in the low crystallinity environment near the nanoparticle surface; the excitation peaks at 273 nm and 303 nm correspond to the $4f5d$ transition of Tb^{3+} ions located in the high crystallinity environment inside the nanoparticles. In samples with small particle size (e.g., 5 nm), most Tb^{3+} ions locate at close to the surface. In this case, the 235 nm peak is very strong, and the 273 nm and 303 nm peaks are rather weak. As the particle size increases, the surface area-to-volume ratio decreases, and the number of Tb^{3+} ions distributed at the surface decreases. These changes result in the decreased intensity at 235 nm and the increased intensity at 273 nm and 303 nm.

In order to test the conclusion above, the emission spectra for 10 nm Y_2O_3:Tb^{3+} ($X = 0.01$) sample under 235 nm and 273 nm excitation were measured as shown in Figure 5. It was found that the emission spectral profiles corresponding to the $^5D_4 \rightarrow {}^7F_J$ ($J = 6, 5, 4, 3$) transition are dependent on the excitation wavelength, indicating that different wavelengths of excitation light excited different Tb^{3+}-occupied sites at or near the surface and inside the nanoparticles. It was also found that the emission spectra under 273 nm excitation exhibit clear spectral slits for each peak; we believe these spectra are mainly due to the emission of Tb^{3+} occupying sites with high crystallinity. The emission spectra under 235 nm excitation are different; we believe these spectra are mainly due to the contribution of the Tb^{3+} located at or near the surface of the nanoparticles.

3.3. Host Absorption Band of Y_2O_3

Figure 6(a) displays the excitation spectra of Y_2O_3:Tb^{3+} (28 nm) doped with different concentrations of Tb^{3+}, while monitoring the $^5D_4 \rightarrow {}^7F_5$ transition. From this figure it can be seen that the relative intensity of the host absorption band of Y_2O_3 increases as Tb^{3+} concentration decreases. Figure 6(b) shows the excitation spectra measured under the same condition for bulk samples, and the same trend was observed for the host absorption band. This is because the energy transfer efficiency from complex exciton to luminescent center is very low. When the concentration of luminescent centers (Tb^{3+}) decreases, more Tb^{3+} ions can capture the transferred energy, and the luminescent center has a higher probability of obtaining the energy from the Y_2O_3 exciton combination. For a certain Tb^{3+} ion, its absorption section of $4f5d$ transition is independent of the doping concentration, thereby with the increase of doping concentration the excitation peak corresponding to the $4f5d$ transition increases, and the relative intensity of the host absorption band of Y_2O_3 decreases relative to the $4f5d$ transition. The same reason can be applied to the case of Y_2O_3:Eu^{3+}. Figure 7 shows the excitation

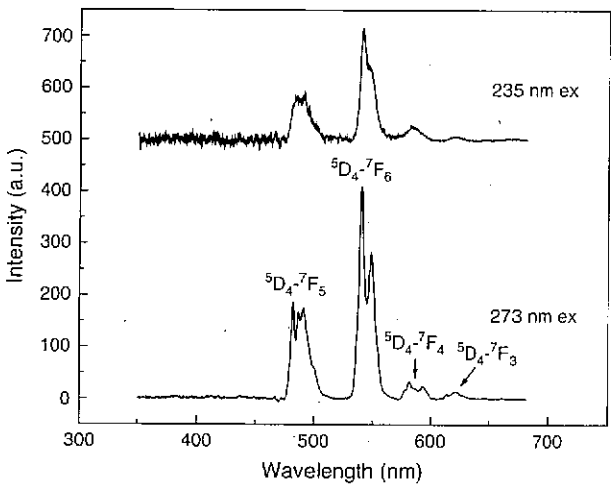

Fig. 5. Emission spectra of the 10 nm Y_2O_3:Tb^{3+} sample ($X = 0.01$) excited by 235 nm and 273 nm UV light. Monitoring scope was 350–680 nm.

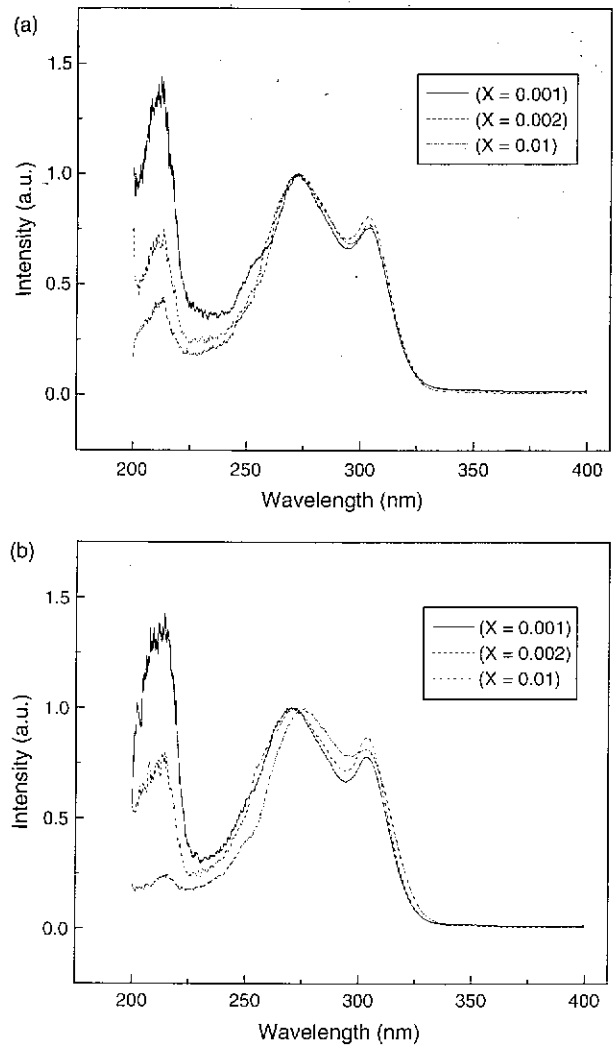

Fig. 6. Excitation spectra of Y_2O_3:Tb^{3+} with different Tb^{3+} concentrations, monitoring the 543 nm emission of the $^5D_4 \rightarrow {}^7F_5$ transition of Tb^{3+} ($X = 0.001$, 0.002, and 0.01). (a) nanoparticle sample (28 nm), (b) bulk sample.

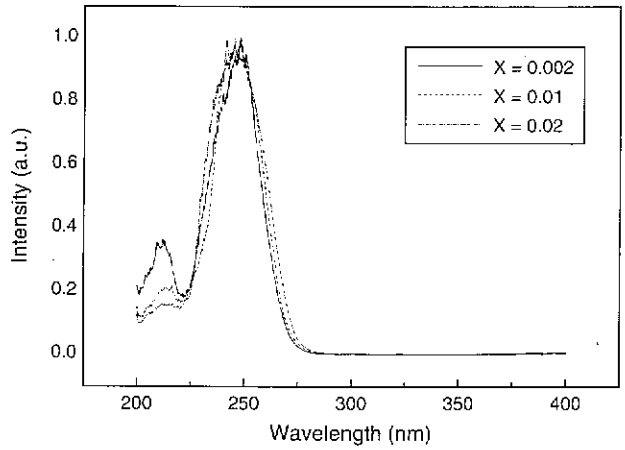

Fig. 7. Excitation spectra of Y_2O_3:Eu^{3+} (30 nm) with different Eu^{3+} concentration, monitoring $^5D_0 \rightarrow {}^7F_2$ transition of Eu^{3+} (611 nm).

spectra for samples Y_2O_3:Eu^{3+} with the same particle size of 30 nm and various doping concentrations. The spectra were normalized to the intensity of the O → Eu CT band. In light of the above analysis, it can be concluded that the excitation efficiency of the Y_2O_3 host absorption band is very low when the Eu^{3+} doping concentration is high and the excitation efficiency will improve if the doping concentration becomes low.

4. CONCLUSIONS

(1) Under the quantum dimension effect and the surface effect, the CT band of Y_2O_3:Eu^{3+} red-shifts obviously. Also, the CT band of the 5 nm sample clearly broadens toward the long wavelength. These facts indicate that the location of the excitation peak of the CT band and the width of the excitation band can be controlled by utilizing the quantum dimension effect and the surface effect.

(2) The profile of excitation spectra for the $4f5d$ band in the Y_2O_3:Tb^{3+} nanocrystals varies when the particle size changes. This is because the Tb^{3+} ions exist in two very different local environments: one is the low crystallinity environment near the surface; the other is the high crystallinity environment inside the particles. The excitation band corresponding to the $4f5d$ transition of Tb^{3+} ions includes contributions from both of these environments and can be differentiated as three peaks at 235 nm and 273 nm, 303 nm. By using the sensitivity of $4f5d$ transition, the Tb^{3+} ions can be used as probe for studying the structure and properties of nanomaterials.

(3) As the Tb^{3+} Eu^{3+} doping concentrations decease, the relative intensity of the excitation peak responsible for the exciton absorption of Y_2O_3, compared to the $4f5d$ transition (or CT band) also increases. The excitation efficiency of the Y_2O_3 host absorption band is very low when the doping concentration of the luminescent center is high. But when the doping concentration is low, the excitation efficiency of Y_2O_3 host absorption band improves. Therefore, the host absorption band may be used for exciting luminescent centers.

References and Notes

1. W. Chen, J. Z. Zhang, and A. G. Joly, *J. Nanosci. Nanotechnol.* 4, 919 (**2004**).
2. W. Chen, J. O. Malm, V. Zwiller, Y. N. Huang, S. M. Liu, R. Wallenberg, J. O. Bovin, and L. Samuelson, *Phys. Rev. B* 61, 11021 (**2000**).
3. W. Chen, R. Sammynaiken, Y. N. Huang, J. O. Malm, R. Wallenberg, J. O. Bovin, V. Zwiller, and N. A. Kotov, *J. Appl. Phys.* 89, 1120 (**2001**).
4. W. Chen, S. Wang, S. Westcott, J. Zhang, A. G. Joly, and D. E. McCready, *J. Appl. Phys.* 97, 835061 (**2005**).
5. J. Zhang, F. H. Su, W. Chen, R. Sammynaiken, S. L. Westcott, D. E. McCready, G. H. Li, and A. G. Joly, *J. Nanosci. Nanotechnol.* 5, 1465 (**2005**).

6. B. J. Sun, H. W. Song, J. W. Wang, H. S. Peng, X. B. Zhang, S. Z. Lu, J. H. Zhang, and H. P. Xia, *Chem. Phys. Lett.* 368, 412 (**2003**).
7. H. W. Song, B. J. Chen, and H. S. Peng, *Appl. Phys. Lett.* 81, 1776 (**2002**).
8. Y. Fang, W. Xu, R. Song, H. Zhang, L. You, J. C. Yu, and H. Liu, *J. Am. Chem. Soc.* 125, 16025 (**2003**).
9. F. H. Su, B. S. Ma, Z. L. Fang, K. Ding, G. H. Li, and W. Chen, *J. Phys.: Condens. Matter* 14, 12657 (**2002**).
10. X. Bai, H. W. Song, L. X. Yu, L. M. Yang, Z. X. Liu, G. H. Pan, S. Z. Lu, X. G. Ren, Y. Q. Lei, and L. B. Fan, *J. Phys. Chem. B* 109, 15236 (**2005**).
11. W. Chen, R. Sammynaiken, and Y. Huang, *J. Appl. Phys.* 88, 1424 (**2000**).
12. H. X. Zhang, C. H. Kam, Y. Zhou, X. Q. Han, S. Buddhudu, Y. L. Lam, and C. Y. Chan, *Thin Solid Films* 370, 50 (**2000**).
13. W. O. Gordon, J. A. Carter, and B. M. Tissue, *J. Lumin.* 108, 339 (**2004**).

Received: 8 March 2007. Accepted: 28 June 2007.

RESEARCH ARTICLE